Atmospheric
Chemistry
and Physics

Supplement of

Examining cloud vertical structure and radiative effects from satellite retrievals and evaluation of CMIP6 scenarios

Hao Luo et al.

Correspondence to: Hao Luo (luoh93@mail2.sysu.edu.cn) and Yong Han (hany66@mail.sysu.edu.cn)
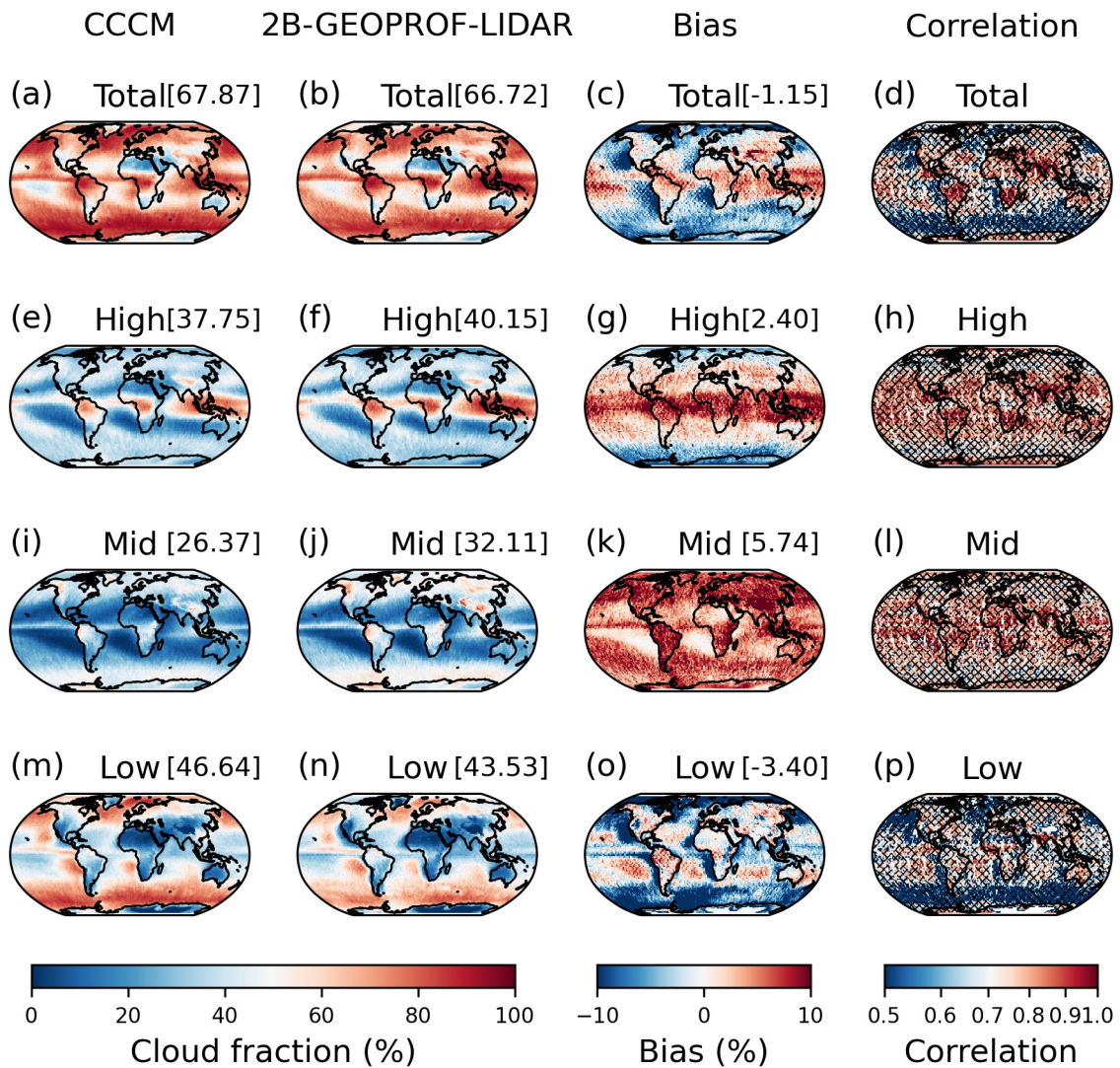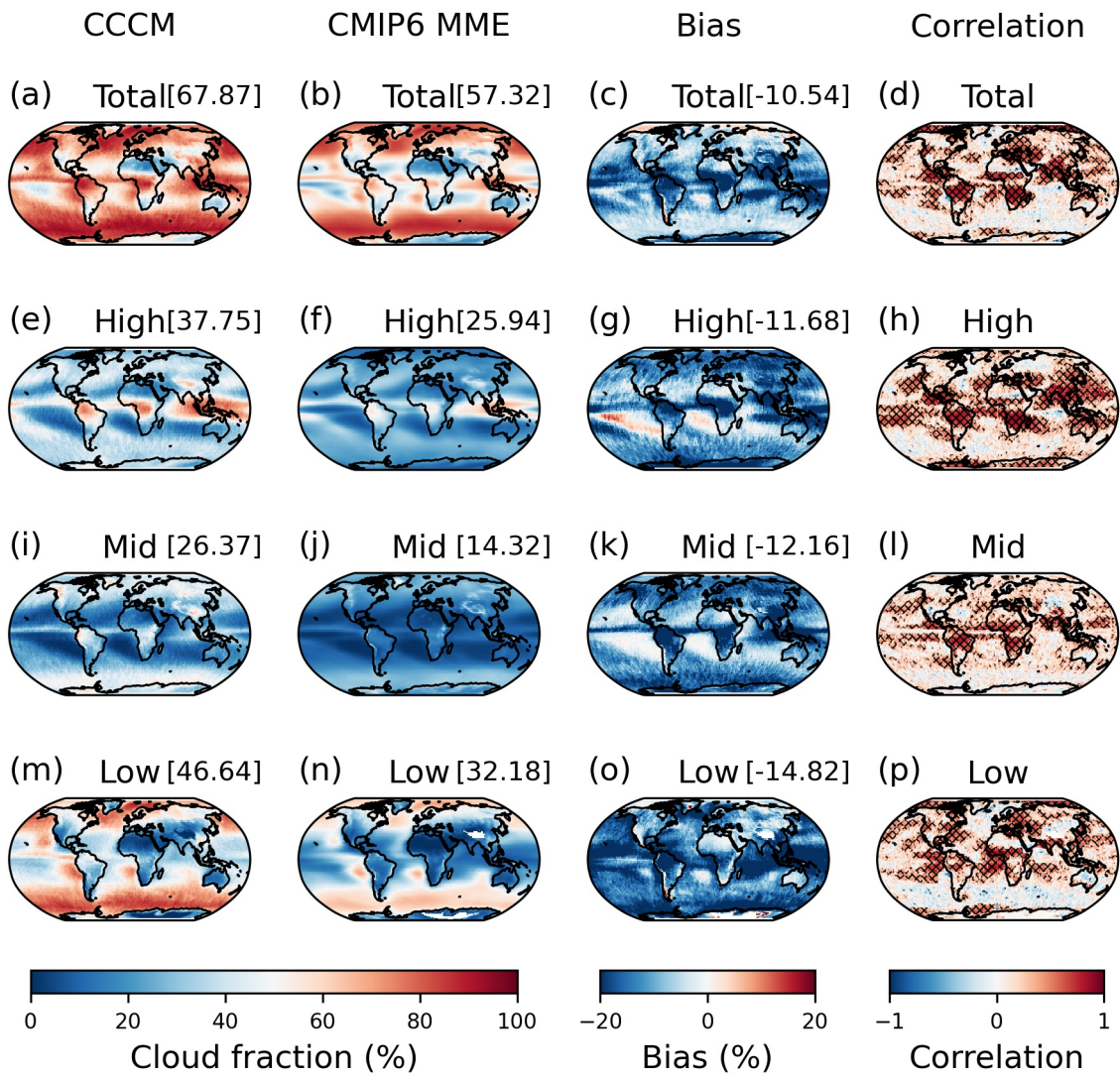
Figure S1: Spatial distributions of the 4-year (2007–2010) average cloud fraction from CCCM and Level 2B GEOPROF-LIDAR, their biases and correlations for the (a–d) total, (e–h) high, (i–l) middle and (m–p) low cloud cover. The bias is defined as GEOPROF-LIDAR minus CCCM. The value above each subfigure denotes the area-weighted global average. Black mesh areas in (d, h, l and p) indicate values passing the 95% confidence level. It should be noted that the cloud types used for the comparison differ from the CVS classes in Sect. 2.3, and they are only categorized into high, middle and low clouds according to the thresholds of 440 hPa and 680 hPa.

Figure S2: Spatial distributions of the 4-year (2007–2010) average cloud fraction of CCCM and eight CMIP6 CALIPSO simulators MME, their biases and correlations for the (a–d) total, (e–h) high, (i–l) middle and (m–p) low cloud cover. The bias is defined as CMIP6 MME minus CCCM. The value above each subfigure denotes the area-weighted global average. Black mesh areas in (d, h, l and p) indicate values passing the 95% confidence level.
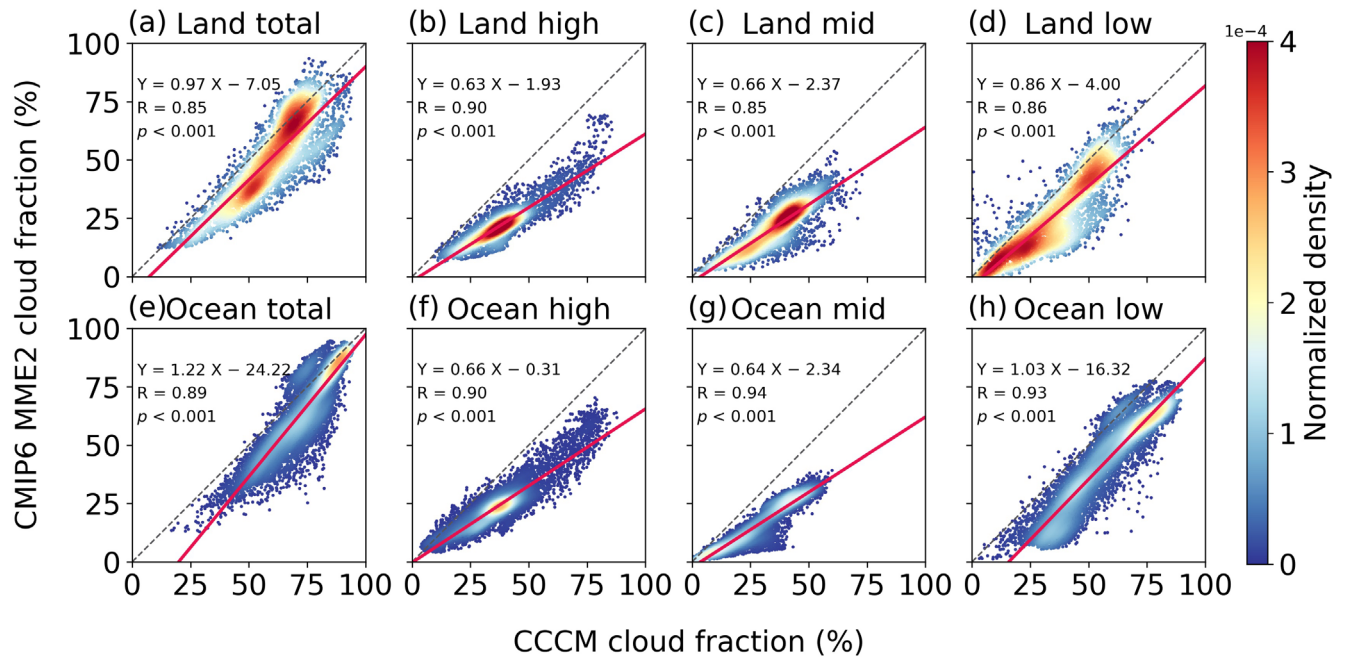
20

25

3
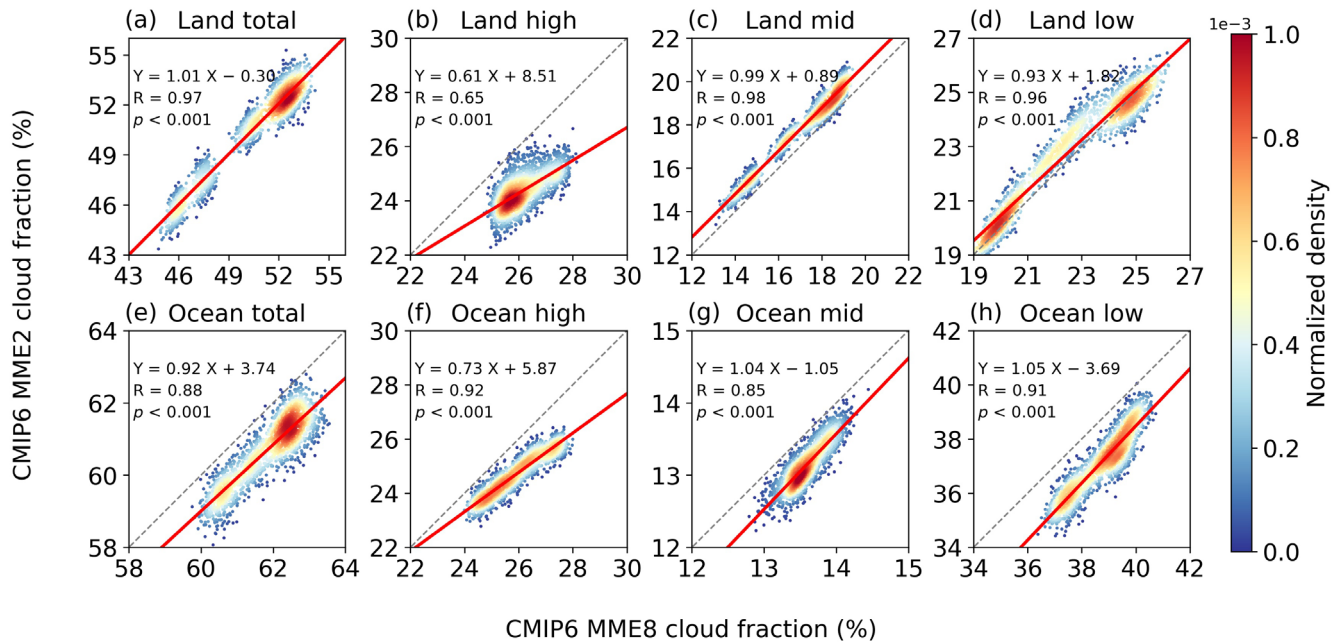
Figure S3: Normalized density plots of 1850–2014 monthly average (a and e) total, (b and f) high, (c and g) middle and (d and h) low cloud fractions estimated from the two CALIPSO simulators MME versus the eight CALIPSO simulators MME over land and ocean, respectively. The regressions are represented by the red lines. The regression function, correlation coefficient (R) and *p* value are given in each subplot.
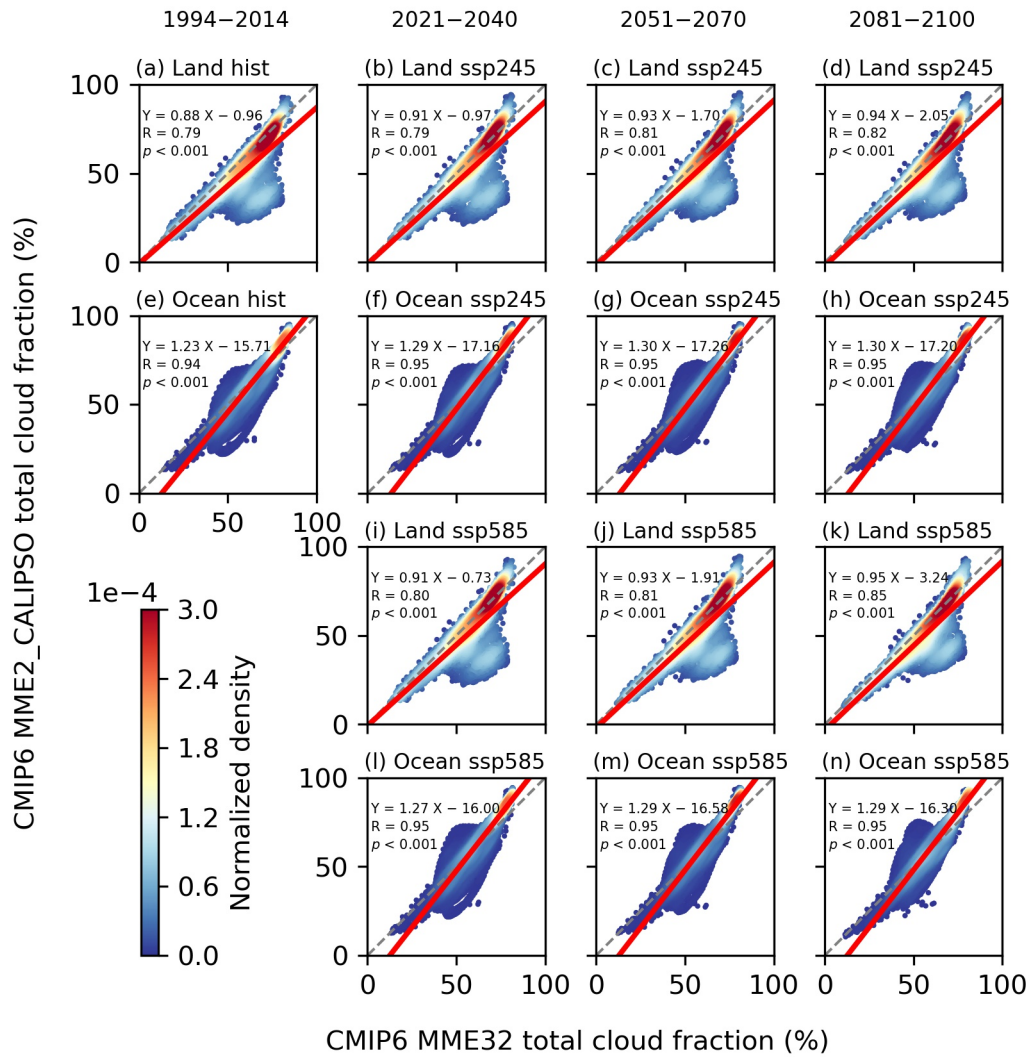
Figure S4: Normalized density plots of monthly average total cloud fraction estimated from the two CALIPSO simulators MME versus the 32 models MME for (a and e) 1994–2014, (b, f, i and l) 2021–2040, (c, g, j and m) 2051–2070 and (d, h, k and n) 2081–2100 over land and ocean, respectively. Two scenarios of (b-d and f-h) ssp245 and (i-n) ssp585 for the future projections are used. The regressions are represented by the red lines. The regression function, correlation coefficient (R) and *p* value are given in each subplot.

Figure S5: Normalized density plots of the 4-year (2007–2010) monthly average (a and e) total, (b and f) high, (c and g) middle and (d and h) low cloud fractions estimated from the two CMIP6 models that employ the CALIPSO simulator (GFDL-CM4 and IPSL-CM6A-LR), as average of the two models, versus the CCCM measurements over land and ocean, respectively. The regressions are represented by the red lines. The regression function, correlation coefficient (R) and p value are given in each subplot.
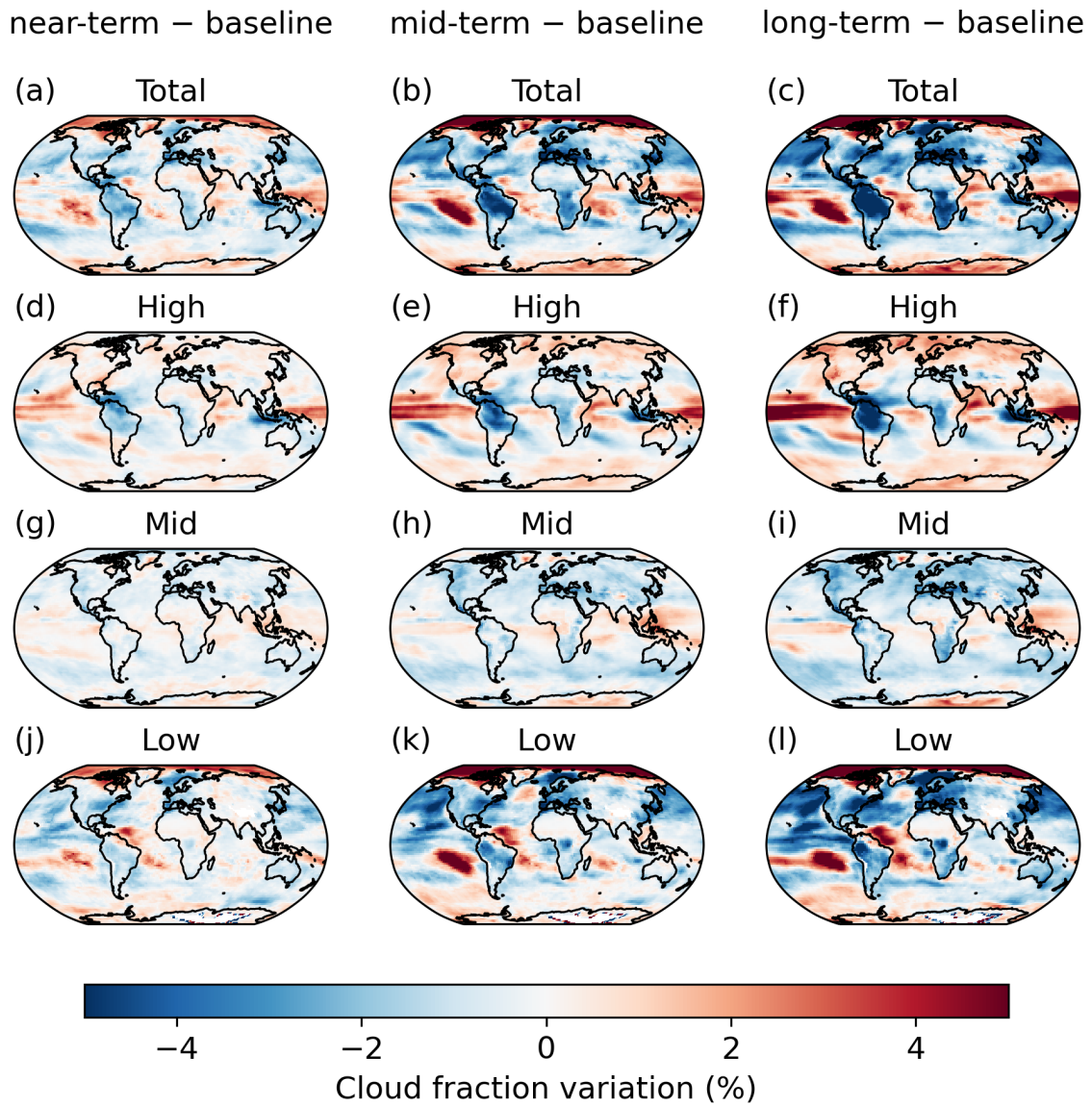
Figure S6: Spatial variations in annual average (a–c) total, (d–f) high, (g–i) middle and (j–l) low cloud fractions in the near-term (2021–2040), mid-term (2051–2070) and long-term (2081–2100) periods compared to baseline (1994–2014) period under ssp245.
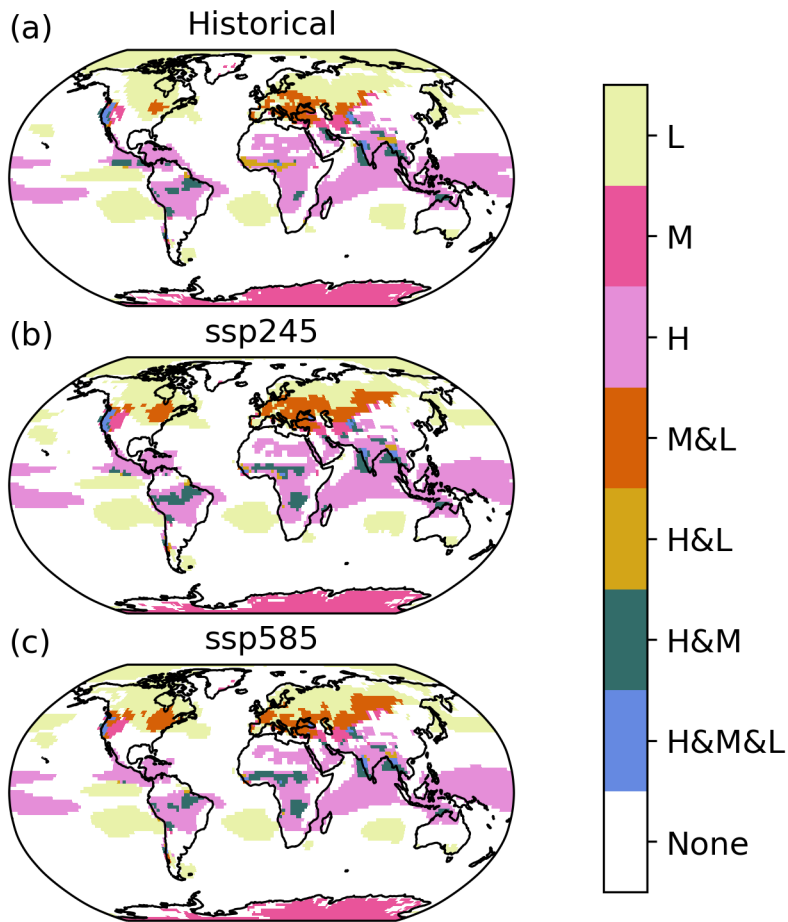
Figure S7: Spatial distributions of the clouds with a positive correlation coefficient >0.9 (p value <0.05) with the total cloud fraction during (a) the historical period (1850–2014) as well as the projected period (2015–2100) under (b) ssp245 and (c) ssp585. The labels 'L', 'M' and 'H' indicate that only one certain cloud type is correlated to the total cloud fraction, while the labels connected by '&' imply that two or three cloud types are simultaneously correlated to the total cloud fraction, and the label 'None' means no cloud is correlated to the total cloud fraction.